Photochemical & Photobiological Sciences (2022) 21:1915–1929
https://doi.org/10.1007/s43630-022-00268-2

ORIGINAL PAPERS

Evaluation of the effectiveness of UV-C dose for photoinactivation of SARS-CoV-2 in contaminated N95 respirator, surgical and cotton fabric masks

Patrícia Metolina[1] · Lilian Gomes de Oliveira[2] · Bruno Ramos[1] · Yan de Souza Angelo[2] · Paola Minoprio[2] · Antonio Carlos Silva Costa Teixeira[1]

Received: 21 March 2022 / Accepted: 4 July 2022 / Published online: 21 July 2022

Abstract

As part of efforts to combat the Covid-19 pandemic and decrease the high transmissibility of the new coronavirus, SARS-CoV-2, effective inactivation strategies, such as UV-C decontamination technologies, can be reliably disseminated and well-studied. The present study investigated the susceptibility of a high viral load of SARS-CoV-2 in filtering facepiece respirators (FFR) N95, surgical mask, cotton fabric mask and N95 straps under three different doses of UV-C, applying both real-time PCR (qPCR) and plaque formation assays to quantify viral load reduction and virus infectivity, respectively. The results show that more than 95% of the amount of SARS-CoV-2 RNA could be reduced after 10 min of UV-C exposure (0.93 J cm^{-2} per side) in FFR N95 and surgical masks and, after 5 min of UV-C treatment (0.46 J cm^{-2} per side) in fabric masks. Furthermore, the analysis of viable coronaviruses after these different UV-C treatments demonstrated that the lowest applied dose is sufficient to decontaminate all masks (~ 3-log_{10} reduction of the infective viral load, > 99.9% reduction). However, for the elastic strap of N95 respirators, a UV-C dose three times greater than that used in masks (1.4 J cm^{-2} per side) is required. The findings suggest that the complete decontamination of masks can be performed effectively and safely in well-planned protocols for pandemic crises or as strategies to reduce the high consumption and safe disposal of these materials in the environment.

Graphical abstract

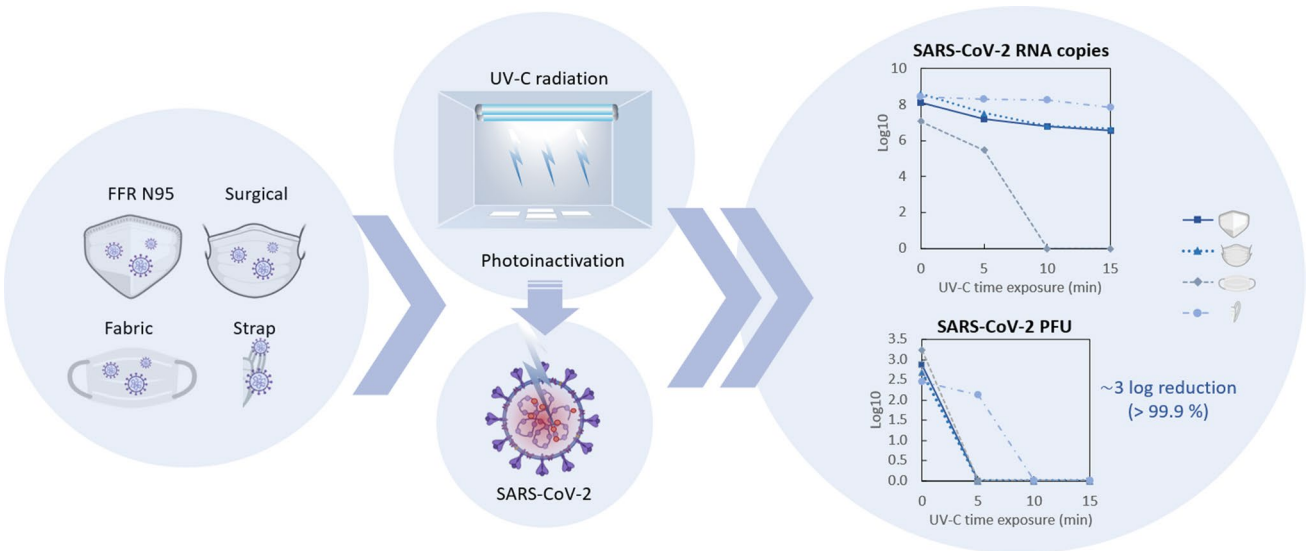

Extended author information available on the last page of the article

Keywords SARS-CoV-2 coronavirus · Covid-19 · UV disinfection · Personal protective equipment reuse · Real-time PCR · Plaque-forming units (PFU)

1 Introduction

The global pandemic Covid-19 caused by the severe acute respiratory syndrome coronavirus 2 (SARS-CoV-2) has led to a widespread crisis in the healthcare system. The high demand for personal protective equipment (PPE) resulted in a deficit of these essential materials, especially N95 filtering facepiece respirators (FFRs) in the initial period of the pandemic [1]. Although the recommendation for FFRs is single use [2], emergency solutions have been adopted to decontaminate and enable the reuse of these devices during the shortage. This strategy should allow for ensuring suitable protection, reducing the high risk of infection by front-line healthcare professionals, since the main route of virus transmission occurs through contact, droplet and aerosol [1, 3]. The crisis highlighted the need for studies that support the adoption of safe and effective guidelines for applying mask decontamination methods in similar situations.

Several methods have been applied to inactivate microorganisms including water and soap, ethanol, isopropyl alcohol, warm moist heat, dry heat or autoclave, bleach, ethylene oxide gas, liquid hydrogen peroxide, vaporous hydrogen peroxide, ultraviolet-C radiation (UV-C), microwave-generated steam and gamma irradiation, among others [4, 5]. For decontamination of FFRs, these procedures needed to be effective against the target microorganism, maintain the integrity and functionality of the filtering properties, leave no hazardous residue for users, and be low-cost, fast-acting, easy to use and readily available [4, 6, 7]. Considering these criteria, UV-C, vaporous hydrogen peroxide and steam methods have been recommended by the Centers for Disease Control and Prevention (CDC), and Occupational Safety and Health Administration (OSHA) for limited reuse of N95 FFRs [8].

Particularly, UV-C radiation has been applied to several processes of decontamination of water, air and sterilization of airborne pathogens in hospital settings. UV-C radiation (100–280 nm) damages the genetic material of the microorganisms by the photooxidation of nucleic acids and the generation of reactive oxygen species (ROS), inactivating viruses and bacteria in general [9, 10]. Coronaviruses and influenza viruses are considered analogous by comprising a single strand of encapsulated RNA (ssRNA). Studies have revealed that these respiratory viruses are more susceptible to UV irradiation compared to other microorganisms [8, 11–13]. However, the UV efficacy depends on the environment, the material, as well as the soiling agent in which the microorganisms are embedded in the material (e.g., saliva or skin oil in masks).

Due to the considerable increase in the use of PPEs during the pandemic, the World Health Organization has reported concerns about the amount of waste produced by their irregular disposition. Approximately one-third of these wastes (2019 data), including medical masks in healthcare facilities around the world are discharged untreated into the ecosystem, posing a serious threat to human health and the environment [14]. WHO thus warns about the urgent need to improve waste management practices and the development of safer and environmentally sustainable innovative solutions, in addition to paying attention to the climate impacts of incineration [14]. These implications make UV-C-based technologies a promising solution to be considered in the decontamination of PPEs, as they are environmentally friendly, practical and can be carried out locally.

Since the advent of the H1N1 influenza pandemic in 2019, the application of UV-C in FFR for reuse has been investigated as a short-term solution for the depletion of the personal protective equipment (PPE) supply chain [15, 16]. The summary of studies involving the susceptibility of encapsulated viruses to UV-C in FFR is shown in Table 1. According to these findings, the minimum UV-C fluence required to achieve a considerable decrease in the viruses ($\geq$ 3-$\log_{10}$ reduction) in FFRs is 1.8 J cm^{-2}. This value corresponds to 100–1000 times higher than the doses used to decontaminate these microorganisms on non-porous surfaces and in the air [10, 13, 17], which emphasizes the need for a careful assessment of the required UV-C dose for different materials.

In addition, substantial work has been reported on maintaining the filtering functionality of FFRs exposed to UV-C radiation. Studies associated with National Institute for Occupational Safety and Health (NIOSH, USA) evaluated several parameters, such as the quality of the physical structure, aerosol filtering capacity, airflow resistance, fitting characteristics, odor, comfort or ease of placement, of the N95 FFRs and demonstrated that even after exposure to several consecutive treatments and using more aggressive doses of UV-C (3.46 J cm^{-2}), the properties of the masks remained unchanged [15, 26–29]. Based on the satisfactory UV-C dose of 1.8 J cm^{-2} obtained to inactivate the influenza virus, Heimbuch et al. [6] suggest that "dozens" of UV-C treatment cycles can be applied without affecting the performance of FFRs.

These considerations reporting the advantages of UV-C disinfection treatment provide important directions for a viable application of this method for the reuse and control of the demand and disposal of these PPEs when necessary. However, investigations are still needed to validate the UV-C

Table 1 Summary of the studies reporting the UV-C photoinactivation of encapsulated viruses in FFR

Virus	FFR material type	Method used as soiling agent/virus carrier	UV-C source	UV-C dose (J cm^{-2})	Irradiance (mW cm^{-2})	Results	References
H1N1	N95 FFRs (6 models)	H1N1 virus was diluted in mucin buffer (concentration of 8 log_{10} $TCID_{50}$ mL^{-1}) and applied as aerosol or droplets to the FFRs	UV-C (254 nm) 80 W lamp (120-cm)	Average of 1.8	1.6–2.0	The virus was reduced to below the limit of detection (> 4- log_{10} reduction) in all FFRs No observable physical deterioration or deformation in FFRs after UV treatment	[6]
H5N1	N95 FFRs (2 models)	H5N1 virus was applied with aerosolized droplets (concentration of 5.5 log_{10} $TCID_{50}$ mL^{-1}) to the FFRs	UV-C (254 nm) 15 W dual-bulb lamp (126 (L) × 15.2 (W) × 10.8 cm (H))	Average of 1.8	1.6–2.0	The virus was considerably reduced (> 4-log_{10} reduction) in both FFRs The qRT-PCR assay indicated a significant reduction in lower levels of detectable viral RNA No profound reduction in filtration performance in the FFRs after UV treatment	[7]
H1N1	N95 FFRs (12 models) and straps (3 models)	H5N1 virus was applied with artificial saliva (mucin buffer) or artificial skin oil (sebum) (concentration of 7 log_{10} $TCID_{50}$) to four areas of the FFRs and straps	Eight 254-nm UV-C lamps (32 in) were placed inside a custom device	1.1	17	The virus was considerably reduced (≥ 3-log_{10} reduction) for both soiling agents in all FFRs and straps Decontamination is dependent on the model type of N95 respirators	[18]
H1N1 H5N1 H7N9 MERS-CoV SARS-CoV-1	N95 FFR	Each type of virus with the indicated concentrations: H1N1 (7.25 log_{10} $TCID_{50}$ mL^{-1}) H5N1 (7.25 log_{10} $TCID_{50}$ mL^{-1}) H7N9 (7.00 or 7.25 log_{10} $TCID_{50}$ mL^{-1}) MERS-CoV (8.00 log_{10} $TCID_{50}$ mL^{-1}) SARS-CoV-1 (8.25 log_{10} $TCID_{50}$ mL^{-1}) were applied with artificial saliva (mucin buffer) or artificial skin oil (sebum) to circular coupons of FFRs	UV-C (254 nm) 20 W bench lamp	1.0	2.3	No detectable virus for either soiling agents (≥ 3.95- log_{10} reduction)	[19]

Table 1 (continued)

Virus	FFR material type	Method used as soiling agent/virus carrier	UV-C source	UV-C dose (J cm^{-2})	Irradiance (mW cm^{-2})	Results	References
SARS-CoV-2	N95 FFRs (5 models) and straps	SARS-CoV-2 virus (concentration of 8×10^7 $TCID_{50}$ mL-1) was applied to four areas of the FFRs and straps	Four UV-C (254 nm) lamps (22 in × 10 in × 8 in)	1.5	16–25	The coronavirus was reduced to below the limit of detection (≥ 3-log_{10} reduction) for two models of FRRs and two models of straps used However, some parts of the facepiece from three FRR models and some straps had a virus concentration above the limit of detection, requiring further disinfection	[20]
SARS-CoV-2	N95 FFR	SARS-CoV-2 (~ 2.5 × 104 $TCID_{50}$ mL^{-1}) were applied to discs from FFRs	LED high power UV germicidal lamp (260–285 nm)	0.33, 0.99 and 1.98	0.55	The coronavirus was considerable reduced (~ 3-log_{10} reduction) at the highest UV-C dose Filtration performance was maintained after three rounds	[21]
SARS-CoV-2	N95 FFR (3 models)	Pooled clinical samples of SARS-CoV-2 were applied to FFRs	UV-C (254 nm) 30 W lamp	0.63	0.32	The presence of SARS-CoV-2 (RT-PCR) and virus viability was considerably reduced for only one model of FFR	[22]
SARS-CoV-2	N95 FFR	SARS-CoV-2 virus (6.35 PFU mL^{-1} (log_{10})) was applied as a single drop and spread in the FFR surface	Pulsed xenon ultraviolet (PX-UV)	Not specified	Not specified	The coronavirus was considerable reduced (< 1.56 PFU/mL (log_{10}), or a > 4.79-log_{10} reduction)	[23]
SARS-CoV-2	N95 FFR (2 models)	SARS-CoV-2 virus (concentration of 8×10^7 $TCID_{50}$ mL^{-1}) in droplets were applied to four areas of the FFRs and strap	UV-C LEDs (272 nm), outputs of 100 mW or 140 mW	0.45–1.6	1.5–3.0	There was an average reduction in viable coronaviruses (> 3-log_{10} reduction) However, the effectiveness of decontamination depends on the contaminated region and the FFR model	[24]
SARS-CoV-2	N95 FFR	SARS-CoV-2 virus (10^6 plaque-forming units (PFU)) were applied on the FFR	Two UV-C (254 nm) lamps	1.3	At least 5.43	Infectious SARS-CoV-2 was not detected by plaque assays (minimal level of detection of 67 PFU mL^{-1}), suggesting a 3.5-log_{10} reduction)	[25]

dose required for effective inactivation of different respiratory viruses on mask surfaces to develop reliable protocols and regulatory management. Additionally, current studies have not yet evaluated the UV-C dose necessary for the considerable decrease in the viral load of SARS-CoV-2 in association with the reduction of its infectivity. In this context, the present study aims to investigate the susceptibility of SARS-CoV-2 to UV-C disinfection of N95 respirators and to extend the evaluation to other masks typically used during a pandemic (surgery and fabric mask), a subject still little explored in the literature. Thus, three different doses of UV-C were studied to assess the minimum exposure required for decontamination, using as measurements the amount of viral load assessed by real-time PCR (qPCR) and plaque formation.

2 Materials and methods

2.1 Assembly and characterization of UV-C device

The UV-C disinfection device consists of a closed cabinet (dimensions 50 × 25 × 35 cm), containing four low-pressure mercury vapor UV tubular lamps, two lamps with a length of 287 mm and a diameter of 16 mm (HNS G5, Osram Inc.), electrical power of 8 W (nominal UV-C of 2 W); and two lamps with a length of 412.2 mm and diameter of 16 mm (TUV FAM, Philips Co.), power of 20 W (nominal UV-C of 6 W), as illustrated in Fig. 1A and B. The emission spectrum of the set of lamps is shown in Fig. 1D. This arrangement proved to be suitable for experimentation in the Biosafety Level-3 (BSL-3) laboratory, allowing a reduced time for irradiation treatments and, consequently, avoiding long exposure to the biological risk of researchers and large expenses with PPE.

For evaluating the homogeneity of the radiation dose necessary for viral inactivation and for defining the regions inside the cabinet for disposing of the samples to be disinfected, measurements of UV-C irradiance and the stability of the lamp intensity were evaluated using a spectroradiometer (SPR-4002, Luzchem). Accordingly, the lower inner surface of the cabinet was divided into 12 rectangles and irradiance measurements were performed at the center of each division. The irradiation map was thus generated by interpolation of measurements using mathematical software (Matlab R15a, Mathworks Inc.). The region used for the experiments is highlighted in Fig. 1B and C, selected for presenting the highest and most homogeneous UV-C intensity.

2.2 Virus isolation and stocks

The procedures were performed in a Biosafety Level-3 (BSL-3) laboratory at the Scientific Platform Pasteur-USP. The respiratory sample (bronchoalveolar secretion) used for viral isolation and obtention of viral stocks was acquired during the acute phase of infection and complying with the inclusion criteria for clinical suspicion of associated viral infection to SARS-CoV-2 adopted by the Brazilian Ministry of Health. For initial viral isolation, Vero CCL81 cells were seeded (2.3×10^6 cells) in T25 tissue culture flasks and maintained in a 37 °C, 5% CO_2 incubator atmosphere overnight before the viral infection. The initial inoculum (passage 1) was prepared to dilute the clinical sample (SPPU-1504, GenBank MW441769) (1:5) in non-supplemented Dulbecco's modified Eagle medium DMEM low glucose. Consecutively, the inoculum was added to the flask and maintained for 1 h at 37 °C. The inoculum was then removed, and cells were washed two times with warm phosphate-buffered saline (PBS) before replenishing with fresh DMEM low glucose media supplemented with FBS (2%) and penicillin/streptomycin (1%, 10,000 U mL^{-1}). The cell culture was then observed for a cytopathic effect on each day after the inoculation. When a prominent cytopathic effect was observed, the cell culture supernatant was collected, centrifuged for the removal of debris (500 g), and stored at − 80 °C as the first viral passage. The same strategy was employed three times to obtain a fourth passage isolate, which was used for mask contamination experiments. The viral stocks used in this study were titrated by plaque-forming unit (PFU) assay.

2.3 UV-C photoinactivation of masks spiked with SARS-CoV-2

Straps (1 cm) and snips (1 × 1 cm) from N95, surgical and cotton fabric masks were contaminated with 1×10^5 PFU of the isolated SARS-CoV-2 strain SPPU-1504. The masks clippings and strap flaps subjected to UV-C treatment were placed in the region of highest irradiance inside the disinfection cabinet (3.0 ± 0.1 mW cm^{-2}) for 5 min (0.46 J cm^{-2} per side), 10 min (0.93 J cm^{-2} per side) and 15 min (1.39 J cm^{-2} per side). In parallel, non-photoirradiated (NP) samples spiked with SARS-CoV-2 were kept inside the biological safety cabinet for 15 min (maximum irradiation time) to assess whether this period per se would decrease viral infectivity.

After these procedures, masks and straps, previously inactivated or not, were submerged in DMEM low media without supplementation for 5 min at room temperature to extract the viral inoculum. This media was then used for RNA extraction and plaque-forming unit assay to confirm the inactivation. The sequence of the experimental procedures is shown schematically in Fig. 2. All experiments were performed in three independent replicates. In addition, the RT-qPCR and PFU assays were performed in duplicates, whose results were averaged for each of the independent experiments.

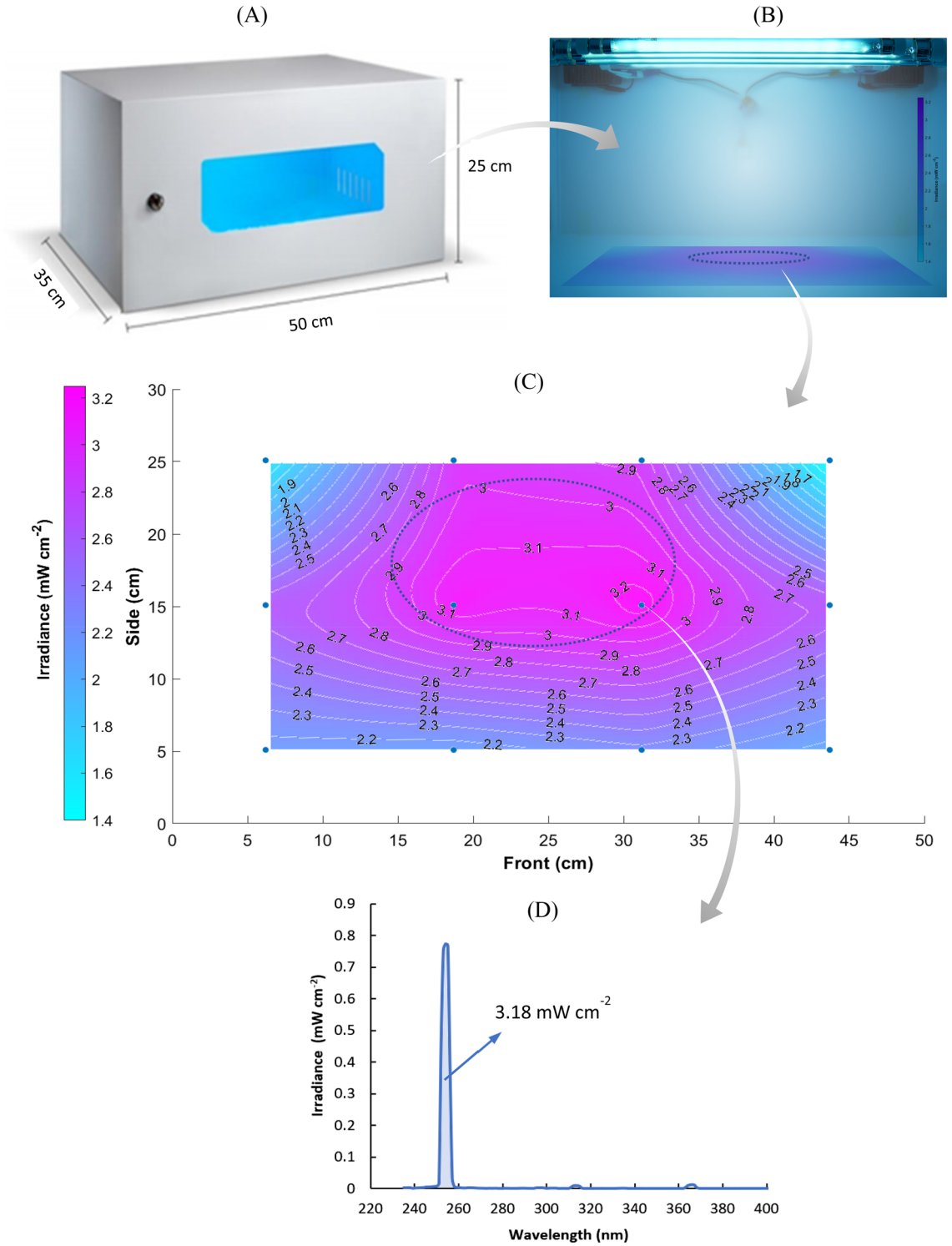

Fig. 1 UV-C disinfection device. **A** Dimensions. **B** Irradiance generated by the four UV-C lamps inside the device. **C** Irradiance surface and contour plot by interpolation of measurement data showed by the points (filled circles). The highest intensity region has an irradiance of 3.0 ± 0.1 mW cm^{-2}. **D** UV emission spectrum presenting the irradiance determined between 251 and 257 nm

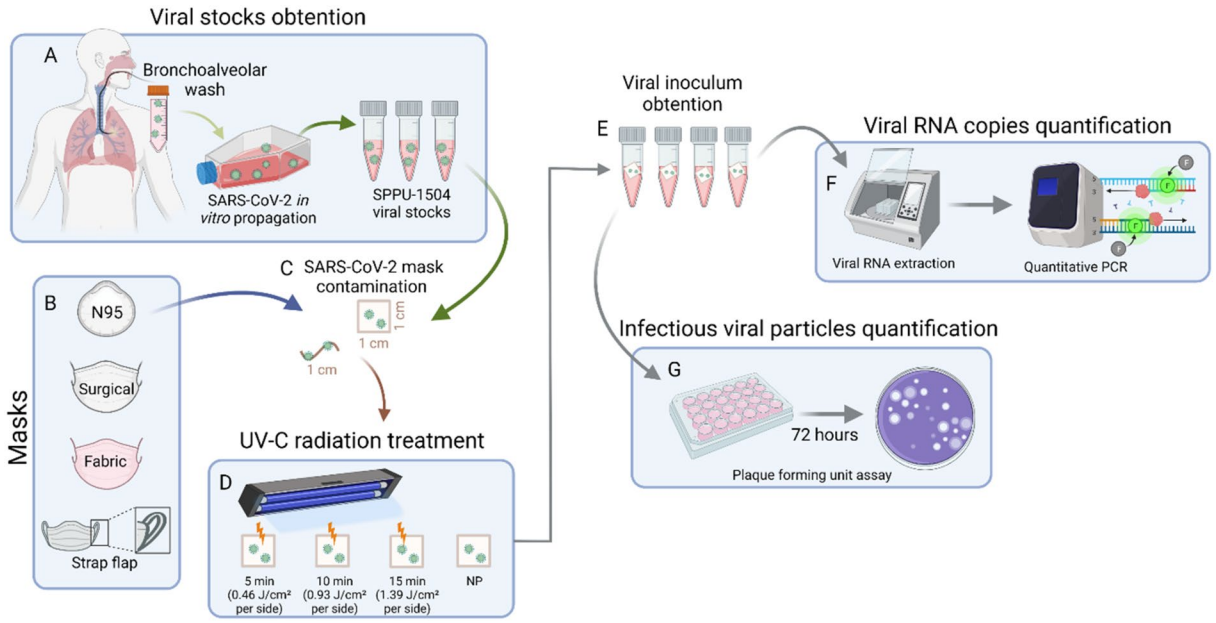

Fig. 2 Schematic description of experimental procedures. **A** To obtain the high viral load stocks of SARS-CoV-2, bronchoalveolar lavage samples from a patient infected with SARS-CoV-2 in vitro were propagated. This stock was used to contaminate N95, surgical and fabric mask clippings (1 × 1 cm) and strap flaps (1 cm) (**B** and **C**). The contaminated snips and strips were then treated with different UV-C exposure times (**D**). Finally, the clippings were immersed in 500 µL of culture medium to obtain the remaining virus (**E**). The virus-containing medium was then used to assess viral RNA and viable viral particles by quantitative PCR and plaque-forming unit assay. *NP* non-photoirradiated

2.4 Plaque-forming unit assay

Vero CCL81 (kindly donated by Prof. Dr. José L. P. Modena—UNICAMP, Brazil) was cultured in DMEM media (low glucose) supplemented with 10% fetal bovine serum (FBS) and 1% penicillin/streptomycin at 37 °C in a fully humidified atmosphere containing 5% CO_2. For virus titration, 1.0×10^5 cells/well were plated in 24 well plates one day before the infection for adhesion. Viral stocks of the SPPU-1504 strain or culture media containing the virus from contaminated masks (inactivated or not) were serially diluted and inoculated in the cell monolayer for 1 h at 37 °C. The inoculum was further removed and replaced with DMEM low-glucose containing 2% FBS and 1% carboxymethylcellulose. After 3 days, the media was removed, and the cells were fixed with 3.7% formaldehyde overnight. Cell monolayers were stained with 1% crystal violet for 15 min. The viral titer was calculated based on the count of plaques formed in the wells corresponding to each dilution expressed as plaque-forming units per mL (PFU mL^{-1}).

2.5 RT-qPCR for viral RNA quantification

Viral RNA extraction from media containing masks inoculum was performed using the MagMAX™ Viral/Pathogen II (MVP II) Nucleic Acid Isolation Kit (Catalog number: A48383) (Applied Biosystems) and carried out according to the manufacturer's instructions. Molecular detection of SARS-CoV-2 was performed using the AgPath-ID One-Step RT-PCR Reagents (Ambion, Austin, TX, USA) and specific primers/probes previously described [30]. RT-qPCR reactions consisted of a step of reverse transcription at 45 °C for 10 min, enzyme activation at 95 °C for 10 min, and 50 cycles at 95 °C for 15 s and 60 °C for 45 s for hybridization and extension using the QuantStudio™ 3 Real-Time PCR System (Thermo Fisher Scientific Inc., Waltham, MA, USA) to collect a fluorescence signal at the end of each cycle. The positive control (SP02/BRA isolate) used was kindly provided by the Laboratory of Clinical Virology, Institute of Biomedical Sciences, University of São Paulo [31].

The quantitative assay was performed using a standard curve produced of a 113 bp fragment of envelope gene from SARS-CoV-2 virus [30] inserted in pMA-RQ vector by Invitrogen (ThermoScientific). Plasmid DNA was transfected in electrocompetent bacteria *E. coli* DH5α and positive colonies were chosen based on ampicillin resistance in LB-agar. The midiprep was followed using PureLink HiPure Plasmid MidiPrep Purification Kit (Invitrogen), following the manufacturer's instructions. The DNA was quantified using Qubit™ dsDNA HS Assay Kit (Invitrogen). The plasmid copy number of molecules was calculated based on Avogadro's constant: Copies = (amount mass (ng) × Avogadro's number (6.02×10^{23} bp mol^{-1}))/(length (bp) × 1×10^9 (conversion factor) × 660 (average mass of 1 bp)). Next,

we prepared a serial dilution of the standard curve from 1×10^8/5 µL to 1×10^1/5 µL copies in a log of base 10. The efficiency of amplification was performed by qPCR in the same conditions of the target gene, as previously described. The amplification efficiency for the SARS-CoV-2 envelope primer was determined from the linear slope of the standard curve, the slope value of which is around ~ − 3.8 and $R^2 \geq 0.99$. The RNA quantification was conducted with the following primers: SARS-CoV-2 (E_Sarbeco) forward—ACAGGTACGTTAATAGTTAATAGCGT; reverse—ATATTGCAGCAGTACGCACACA; probe FAM—ACACTAGCCATCCTTACTGCGCTTCG-BHQ1.

2.6 Statistical analysis

To explore potential differences of means between the inactivated viral inoculum versus the masks that were not submitted for inactivation, we used the One-way ANOVA test with Tukey's multiple comparisons where p-adjusted < 0.05 indicated significance. All the graphs and statistical analyses were obtained using GraphPad Prism 8 software. Error bars indicate the standard deviation.

3 Results and discussion

3.1 Characterization of the UV-C irradiation in the disinfection cabinet

Measurements of the UV-C irradiation were taken continuously for 60 min to evaluate the emission dynamics of the light sources. It was observed that the lamps require between 10 and 20 min to stabilize their emission intensity after being turned on at room temperature. After being kept on for a period above 30 min, the maximum emissive power reached by the lamps is not affected when they are turned off for a short time (1 min) and turned back on again. Therefore, it was possible to momentarily turn off the device to collect the irradiated samples without affecting the continuity of the analysis. Regarding the homogeneity of the irradiated field, the mapping of the radiation field inside the sterilization chamber is displayed in Fig. 1C, indicating the region of greatest irradiance with a narrow standard deviation of the UV-C-dose (3.1 ± 0.1 J cm^{-2}).

3.2 UV-C Photoinactivation

The results of the amount of viral load performed by real-time PCR (qPCR) are shown in Fig. 3 and Table 2 for each of the evaluated samples of N95, surgical and cotton fabric masks and straps. As noted, a considerable reduction in the number of viral RNA copies was observed in the three masks after UV-C treatment compared to non-irradiated materials. In contrast, the control runs represented by the NP samples showed a higher number of viral particles and RNA copies compared to the irradiated samples. It can be understood that the observed reduction was caused only by UV-C irradiation. The most effective disinfection occurred in fabric masks, revealing a reduction in the SARS-CoV-2 RNA above 95% after 5 min of photoirradiation (0.46 J cm^{-2} per side) and a reduction below the detection limit (> 99.9%) after 10 min (0.93 J cm^{-2} per side). The surgical mask and FFR N95 also showed considerable inactivation of the genetic material after 5 min and a reduction between 97 and 99% in the amount of viral RNA after 15 min (1.4 J cm^{-2} per side) of photoirradiation. In contrast, the strap samples showed a significant drop in viral genetic material only after 15 min of UV-C treatment, indicating the need for higher doses of UV-C for its decontamination compared to the three mask samples.

The reduction in SARS-CoV-2 RNA copies after decontamination can be considered significant, since the photoinactivation mechanisms due to direct exposure to UV-C is related to damage to genetic material and/or viral proteins [32]. The absorption of UV-C radiation by RNA causes cross-linking of adjacent pyrimidine bases, inhibiting virus replication [9, 32, 33]. Lo et al. [32] found that SARS-CoV-2 spike and nucleocapsid proteins after UV-C exposure maintained their apparent morphology, showing no evident damage. Furthermore, as traditional RT-qPCR analysis detects only a small region of the viral genome, these researchers used a long RT-qPCR, revealing that UV-C irradiation decreases the amount of RNA by 56.6%. This result was strongly correlated with decreased infectivity of the virus, indicating that genome damage was the main inactivation mechanism of SARS-CoV-2 [32]. In our results, the presence of viral RNA even after UV-C irradiation can be explained by the following hypotheses: (1) RNA strains that are not necessarily inside a viable viral particle; (2) The number of layers contained in each mask differently absorb the inoculum containing the virus, and the shadowing effect that can occur in the innermost layers reduce the effectiveness of UV-C radiation; for example, no viral RNA was detected in the fabric mask, which has only one layer; (3) Since the qPCR technique can only recognize a piece of viral RNA, it is also reasonable to consider that UV-C causes cross-linking of RNA from adjacent pyrimidine bases in regions other than that recognized by the SARS-CoV-2 primers used in this study. Most importantly, qPCR does not differentiate viable, infectious coronavirus particles from inactivated ones.

Therefore, to assess the infectivity of SARS-CoV-2, we quantified the remaining viruses after UV-C treatment through plaque-forming assays in masks and strap samples. Figure 4 presents the results for the three types of masks, indicating that the lowest dose of UV-C is effective against

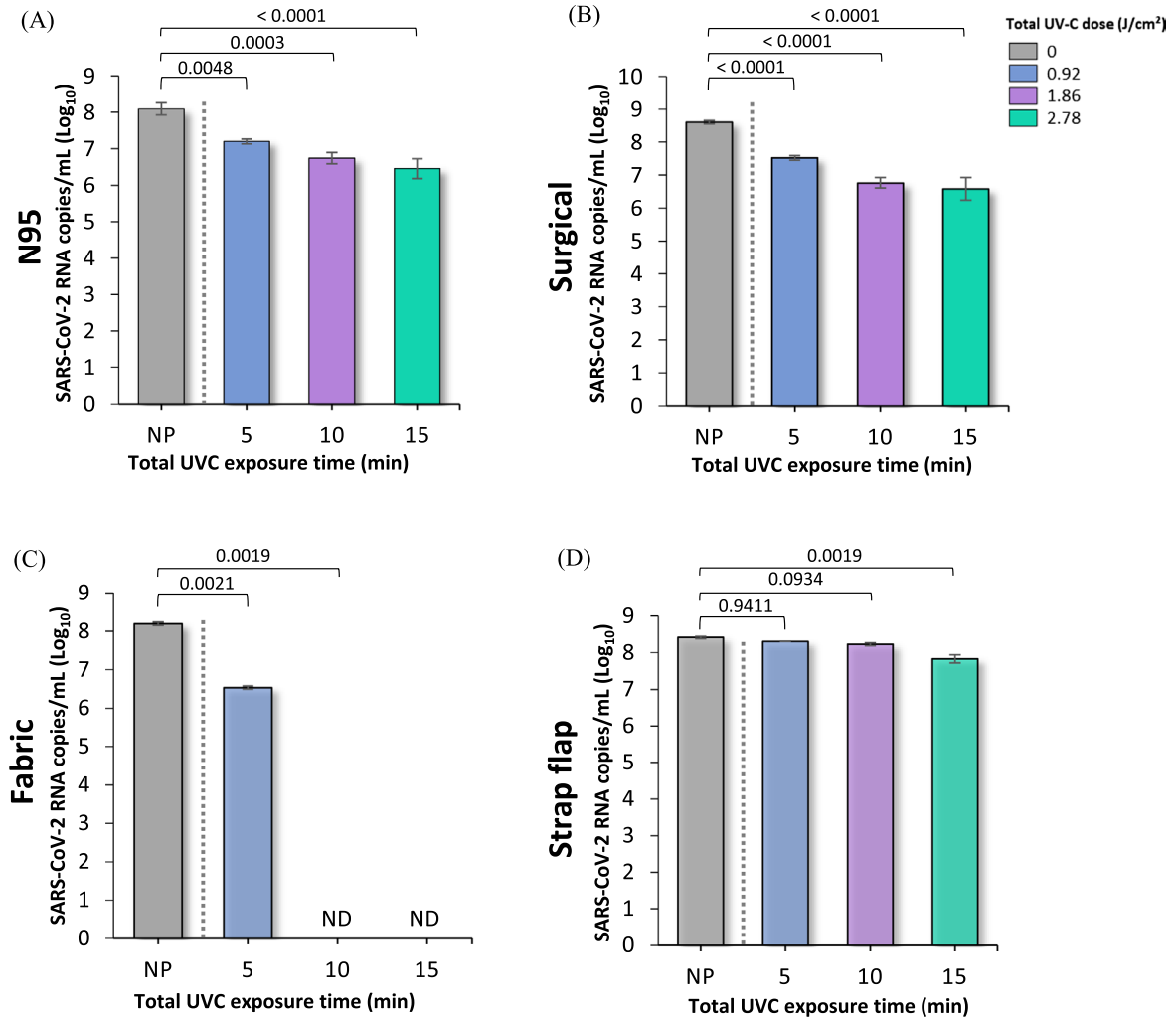

Fig. 3 UV-C disinfection of both sides of SARS-CoV-2 contaminated **A** FFR N95 mask, **B** surgical mask, **C** fabric mask and **D** strap flaps at different treatment times: 5 min (0.46 J cm^{-2} per side), 10 min (0.93 J cm^{-2} per side) and 15 min (1.39 J cm^{-2} per side). Graphs represent viral quantification of SARS-CoV-2 RNA copies by qPCR at log_{10}. Error bars indicate the standard deviation of three independent experiments, except for fabric masks, whose results correspond to two independent measurements. Statistical analysis was performed by one-way ANOVA followed by multiple comparisons between groups using Tukey's test. The *p* values are shown in the horizontal bars above the graphs, considering a significance level $p < 0.05$. *ND* not detected; *NP* non-photoirradiated

SARS-CoV-2, with an undetectable level or ~ 3-log_{10} reduction (or > 99.9% reduction) of the infective viral load. In the case of the straps, a reduction below the detection level is found only after 15 min of UV-C treatment, a dose three times higher than that used in masks (Fig. 4D). This indicates that a reduction of around 70% in the amount of RNA obtained by qPCR (~ 0.56 log_{10} reduction) does not present an infective or viable viral load of the coronavirus. Although N95 FFR, surgical and cotton fabric masks were contaminated with 1×10^5 PFU of SARS-CoV-2, the infectious viruses recovered had an average value of $9.32 (\pm 0.78) \times 10^2$ PFU, i.e., a value two to three orders of magnitude lower than the initial value. This efficiency yield of the extraction procedure is in line with previous results reported for SARS-CoV-2 [25]. Furthermore, using Pearson's correlation test, a significant positive correlation between RNA and PFU was observed in all materials tested. The *p* values of Pearson's correlation for N95, surgical and fabric masks were 0.0039 ($R^2 = 0.9922$), 0.0007 ($R^2 = 0.9985$) and 0.0123 ($R^2 = 0.9996$) (data not shown). According to the literature [34], the characteristic relationship between viral RNA copies and infectious particles can range from 3- to 5-log_{10}, which was also found in our data.

It is important to emphasize that in this study, we used a high load of coronavirus (1×10^5 initial viral inoculum corresponding to 1×10^8 RNA copies mL^{-1} SARS-CoV-2), representing the worst-case mask contamination scenario. According to data reported by Pan et al. [35], clinical

Table 2 Effect of UV-C disinfection of SARS-CoV-2-contamined masks and straps analyzed by real-time PCR (qPCR)

Mask	SARS-CoV-2 RNA copies mL^{-1}				% Reduction		
	Total exposure time				Total exposure time		
	0 min	5 min	10 min	15 min	5 min	10 min	15 min
N95	1.99×10^8	1.89×10^7	8.85×10^6	1.33×10^6	90.5	95.6	99.3
	1.19×10^8	1.62×10^7	4.84×10^6	2.82×10^6	86.4	95.9	97.6
	7.84×10^7	1.30×10^7	3.82×10^6	6.09×10^6	83.4	95.1	92.2
Mean	1.32×10^8	1.60×10^7	5.84×10^6	3.41×10^6	87.9	95.6	97.4
Surgical	4.18×10^8	2.87×10^7	5.03×10^6	1.29×10^6	93.1	98.8	99.7
	3.38×10^8	3.11×10^7	4.17×10^6	7.43×10^6	90.8	98.8	97.8
	4.55×10^8	4.14×10^7	9.48×10^6	5.86×10^6	90.9	97.9	98.7
Mean	4.04×10^8	3.37×10^7	6.23×10^6	4.47×10^6	91.6	98.5	98.8
Fabric	1.42×10^8	3.82×10^6	ND	ND	97.3	> 99.9	> 99.9
	1.71×10^8	3.11×10^6	ND	ND	98.2	> 99.9	> 99.9
Mean	1.57×10^8	3.47×10^6	ND	ND	97.8	> 99.9	> 99.9
Strap	2.86×10^8	2.04×10^8	1.92×10^8	9.99×10^7	28.7	32.9	65.1
	2.39×10^8	2.02×10^8	1.62×10^8	5.63×10^7	15.5	32.2	76.4
	2.55×10^8	1.99×10^8	1.55×10^8	5.7×10^7	22.0	39.2	77.6
Mean	2.60×10^8	2.02×10^8	1.70×10^8	7.11×10^7	22.4	34.7	72.7

ND not detected

[a]The total exposure time is the sum of UV-C exposure time for each side of the mask or strap: 5 min (0.46 J cm^{-2} per side), 10 min (0.93 J cm^{-2} per side) and 15 min (1.39 J cm^{-2} per side)

samples collected from patients with Covid-19 showed that the viral load has a mean of 7.99×10^4 copies mL^{-1} from throat samples and 7.52×10^5 copies mL^{-1} from sputum samples. Evaluating symptomatic cases with very high pharyngeal shedding during the first week of SARS-CoV-2 infection, Wölfel et al. [36] revealed a peak of 7.11×10^8 RNA copies per throat swab. Additionally, the modeling study design by Goyal et al. [37] indicated that coronavirus transmission is more likely when there is exposure to an infected person with a viral load > 10^8 SARS-CoV-2 RNA copies (75% probability) and > 10^7 SARS-CoV-2 RNA copies (39% probability), while the transmission is unlikely with exposure to an infected person with a viral load < 10^5 SARS-CoV-2 RNA copies (~0.002% probability) and very unlikely at an airborne viral load < 10^4 SARS-CoV-2 RNA copies (~0.00005% probability). Therefore, although masks with high contamination should preferably be discarded, decontamination of masks for reuse by UV-C radiation can be considered quite effective even in high contamination situations.

The susceptibility of SARS-CoV-2 to UV-C radiation from our findings is in line with previous studies performed with ssRNA viruses, as summarized in Table 1. Overall, studies report a satisfactory reduction of ≥ 3-$\log_{10}$ units of 50% tissue culture infective dose (TCID50), a measure considered analogous to the PFU assay [34]. Considering the analysis of the viable virus load, the UV-C dose of around 1 J cm^{-2}, the sum of the exposure of the lowest applied dose (0.46 J cm^{-2} per side) is shown enough to inactivate these pathogens in the different mask materials evaluated. As reported in the literature, straps are less effective in disinfection and must be submitted to higher UV-C doses.

More studies should be carried out regarding the microstructural integrity of the masks and the filtering properties of KN95 after UV-C treatment. Previous studies evaluated the fit and filtering capacity in FFRs and the maximum UV-C dose considered in our study is within those evaluated. Viscusi et al. [26] subjected FFRs to ten consecutive UV-C decontamination treatments using less aggressive (0.216 J cm^{-2}) and more aggressive (3.46 J cm^{-2}) exposure conditions to each side of the respirators, reporting no changes in qualitative and penetration level with either treatment. Viscusi et al. [27] revealed that there were no changes in physical appearance, odor, filter aerosol penetration and filter airflow resistance in the FFRs using UV-C radiation (0.176–0.181 J cm^{-2}). Expanding on the previous study, Bergman et al. [15] also verified the maintenance of these same properties after three consecutive UV-C treatment cycles. Using a standard OSHA quantitative fit test, Viscusi et al. [28] evaluated the fitting characteristics, odor, comfort, or donning ease of N95 FFRs, indicating that users would likely have no reduction in fit and unpleasant experiences after UV-C treatment. The study by Lindsley et al. [29] investigated the four models of N95 FFRs under UV-C doses from 120 to 950 J cm^{-2}, showing little effect on particle penetration (up to 1.25%) and flow resistance. However, they observed that the strength of the FFRs materials was considerably reduced at higher UV doses and depends on the models evaluated.

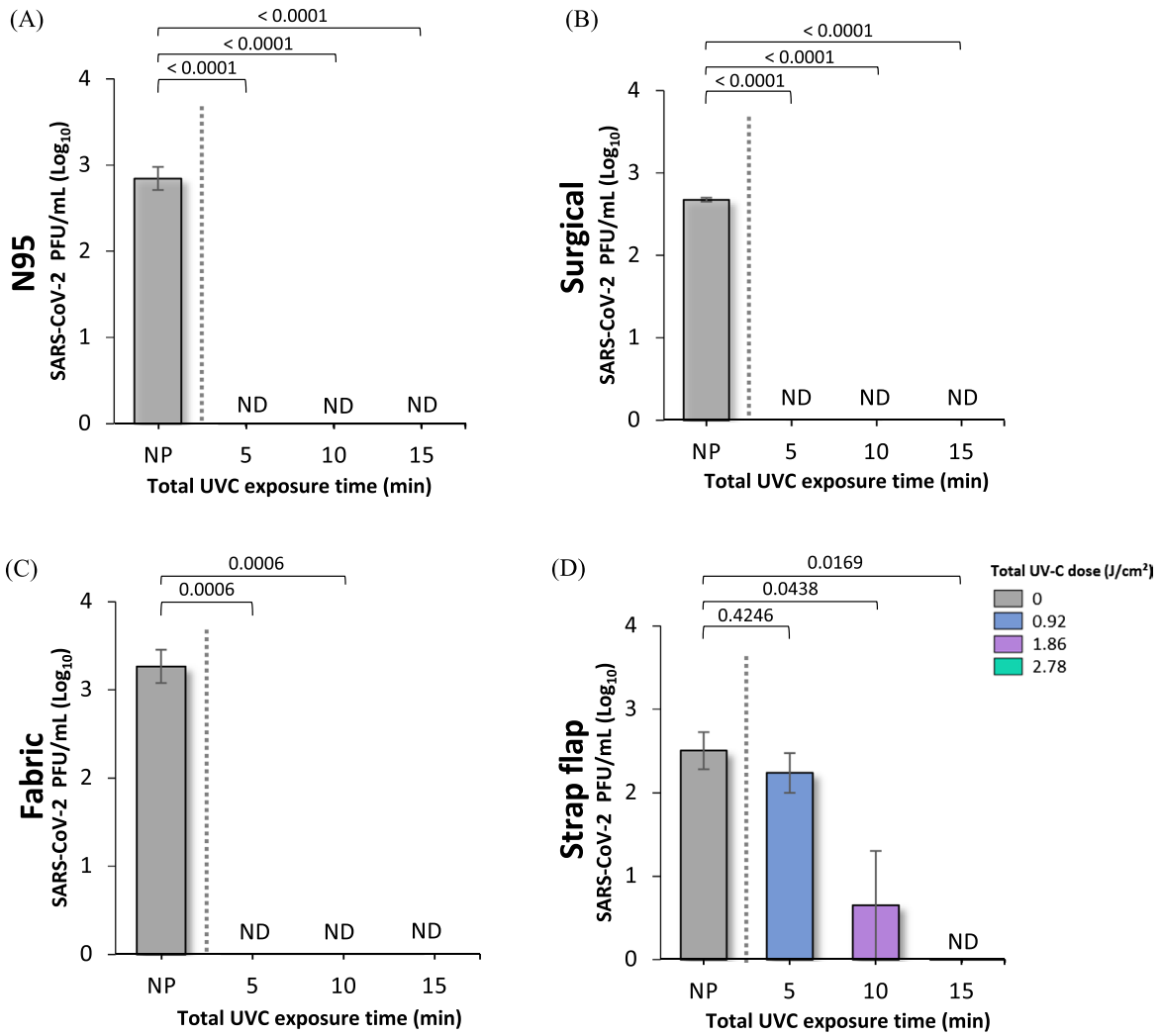

Fig. 4 UV-C disinfection of both sides of SARS-CoV-2 contaminated **A** FFR N95 mask, **B** surgical mask, **C** fabric mask and (**D** strap flaps at different treatment times: 5 min (0.46 J cm^{-2} per side), 10 min (0.93 J cm^{-2} per side) and 15 min (1.39 J cm^{-2} per side). Graphs represent log_{10} infectious viral particles measured by the PFU assay. Error bars indicate the standard deviation of three independent experiments. Statistical analysis was performed by one-way ANOVA followed by multiple comparisons between groups using Tukey's test. The *p* values are shown in the horizontal bars above the graphs, considering a significance level $p < 0.05$. *ND* not detected; *NP* non-photoirradiated

Recent investigations in response to the Covid-19 pandemic have reinforced the assessment of the effects of multiple UV-C disinfection cycles on FFRs. Liao et al. [38] reported that the filtration efficiency of FFRs is maintained after 10 cycles of UV-C treatment and that little degradation occurs by 20 cycles. Ontiveros et al. [39] evaluated two models of FFRs exposed to UV-C doses ranging from 1 to 10 J cm^{-2} per side (10 cycles) and found no significant impact on structural integrity, fit, and filtration efficiency of the respirator and the strength of straps. Conversely, limitations of the UV-C disinfection method pointed out by the researchers are the attenuation of radiation through the porous layers of the respirators and the shadowing caused by materials deposited on the mask surface [20, 24, 39]. Despite this, Huber et al. [40] experimentally evaluated the dose of UV-C irradiation that penetrates the interior of the FFRs, and the inactivation of coronaviruses was modeled using these data. The results indicated that UV-C exposure (0.8–1.2 J cm^{-2}) induces a lower than 3-log_{10}-order reduction and a 2-log_{10}-order reduction of the virus on the surface and the interior of the FFR, respectively. In addition, they reported that a dose 50-fold higher does not affect the filtration or fit of the N95 masks, enabling the treatment to be carried out repeatedly.

It is important to note that the differences found in the disinfection performance of each type of PPE mask are strictly related to the microstructural configuration and the material of which they are manufactured, resulting in shadowing

when exposed to UV-C radiation (see Fig. S1–S4 in the Supplementary Information). The filtering facepiece N95 respirators are composed of a mesh of polypropylene microfibers and electrostatic charges, with high filtering performance, blocking at least 95% of solid and liquid aerosol particles [41], while the surgical mask is fluid-resistant against large respiratory droplets [42]. Although the four-layer constitution (Fig. S1) of the N95 prevents UV-C radiation from penetrating the inner layers, the good filtering capacity of aerosols and the hydrophobic aspect of the respirator mean that most viral particles are concentrated in the outer layers. The effectiveness of UV-C decontamination of the triple-layer surgical masks (Fig. S2) was quite close and slightly better compared to the results with N95. As the straps in the N95 mask have a rougher structure, disinfection is less efficient than in masks (Fig. S4). However, the penetration of UV-C radiation can be improved by keeping the straps tight, increasing the penetration of UV-C radiation inside the elastic loop.

Furthermore, we compared these results with the efficiency of fabric masks made from 100% cotton, which is being commonly used by the population. As shown in Fig. S4, they have a coarser microstructure, composed of twisted and intertwined cotton threads, configured mostly in two layers. Although there is a high absorption of soiling agents containing the coronavirus in the cotton fabric, the lower filtering capacity allows for better penetration of UV-C radiation, making decontamination more efficient compared to the other two PPE.

These results provide the adoption of alternative strategies for the use of masks by the general public, helping to effectively combat the spread of the virus. Medical masks are strongly recommended for use by healthcare professionals, elderly people, people with comorbidities and people with suspected Covid-19 [14]. Hence, in some situations, the safe reuse through UV-C disinfection of these masks presenting a better filtering capacity than fabric masks may be preferable, make it possible to ensure better availability, reduce cost and, secondarily, mitigate the amount of waste due to the widespread disposal of these materials in the current pandemic context.

Based on the increase in studies that address UV-C radiation as an important alternative for microbiological decontamination, more stringent regulations and protocols are still needed for a safe and proven effective practice of the technology for widespread use. With the advent of Covid-19, companies and startups have commercially launched UV-C devices to be used in the disinfection of surfaces and objects in general. However, these products do not usually present clear validation to guarantee that the applied UV-C dose is effective in eliminating different pathogens, mainly influenza viruses and SARS-CoV [43]. Additionally, there is no reliable information on whether these devices are being configured with adequate protection and security against harmful exposure to UV-C radiation by users. In this context, we have also developed a prototype of a continuous device for rapid mask disinfection, whose design and operating mode are briefly described in the Supplementary Information. Decontamination for the reuse of masks would be used as an emergency solution in situations of pandemic crisis (as experienced by Covid-19) and, more importantly, as a relevant decontamination solution for the large number of masks irregularly discarded in the environment, a problem recently pointed out by the WHO [14]. The prototype can be optimized and scalable by adding a greater number of lamps and/or using lamps with higher UV-C power as needed. The effectiveness of the disinfection of PPEs containing SARS-CoV-2 in this continuous device and its optimization is the subject of further investigation, given the constraints associated with the size of the prototype and the analysis of the masks as a whole, which present limitations in terms of experimentation within the Biosafety Level-3 (BSL-3) laboratory. Thus, further studies are needed to validate the results on the full mask and the effect of both surfaces simultaneously exposed to UV-C radiation.

4 Conclusions

The results of this study indicated that SARS-CoV-2 can be effectively inactivated in three different types of masks (FFR N95, surgical and cotton fabric) through UV-C radiation, even in situations with high viral concentrations. Real-time PCR analysis revealed that more than 95% of the amount of SARS-CoV-2 RNA can be reduced after 10 min of UV-C exposure (0.93 J cm^{-2} per side) in FFR N95 and surgical masks, and after 5 min of UV-C treatment (0.46 J cm^{-2} per side) in cotton fabric masks, while 70% of viral RNA is reduced on elastic straps after 15 min of UV-C exposure (1.4 J cm^{-2} per side). Furthermore, the analysis of viable coronaviruses after these different UV-C treatments demonstrated that the lowest applied dose (0.46 J cm^{-2} per side) is sufficient to completely decontaminate all masks. However, for the elastic strap of N95 respirators, a UV-C dose three times greater than that used in masks is required (1.4 J cm^{-2} per side). When examining the mask in detail, the UV-C disinfection treatment was more effective in masks with fewer layers, less particle filtering capacity and consequently greater UV-C penetration, as is the case of cotton fabric masks. Although the reuse of N95 and surgical masks are aimed at critical periods of lack of PPE stock by health professionals, the reuse of masks by the population, especially fabric ones, is a routine practice. Thus, due to the better filtering capacity, reusing decontaminated medical masks may be a preferred alternative to fabric masks in some situations. Furthermore, the treatment of discarded masks

by UV-C is an important practice to be considered in waste management to avoid environmental contamination.

It is worth to emphasize that to make decontamination sustainable, appropriate scale-up studies must be performed to maximize treatment throughput and minimize energy costs. Considering that, for now, the alternative to UV-C decontamination involves incineration and acquisition of new PPE – with all the costs (transport, final destination, taxation), environmental impacts and carbon footprints involved – UV-C can be a sustainable alternative, after proper equipment optimization. Therefore, the findings of UV-C disinfection in different masks allow directing the development of more effective technological alternatives for the reuse of similar medical and non-medical PPE materials, mainly to improve the effectiveness of protection against cross-contamination of pathogens in a quick-effective, low-cost and sustainable manner.

Supplementary Information The online version contains supplementary material available at https://doi.org/10.1007/s43630-022-00268-2.

Acknowledgements The authors express their gratitude to the association "Fundo Patrimonial Amigos da Poli", Escola Politécnica of the University of São Paulo, for the financial support. The authors are indebted to the São Paulo Research Foundation (FAPESP—process # 2017/27131-9), the Institut Pasteur (DI2020-16/18), and the Cooperation and Cultural Action Services of the São Paulo French Consulate (#185BRA1184—2020/SPPU). LGO and YSA received a grant from Coordination for the Improvement of Higher Education Personnel (CAPES) (#88887.423542/2019-00 and #88887.474625/2020-00, respectively).

Declarations

Conflict of interest The authors declare no conflict of interest.

References

1. World Health Organization. (2020). *Modes of transmission of virus causing COVID-19: Implications for IPC precaution recommendations*. https://www.who.int/news-room/commentaries/detail/modes-of-transmission-of-virus-causing-covid-19-implications-for-ipc-precaution-recommendations. Accessed on 3 Dec 2021.
2. Centers for Disease Control and Prevention. (2007). 2007 Guideline for isolation precautions: Preventing transmission of infectious agents in health care settings. Retrieved from https://www.sciencedirect.com/science/article/pii/S0196655307007407?via%3Dihub. 28 Nov 2021.
3. Nardell, E. A. (2021). Air disinfection for airborne infection control with a focus on COVID-19: Why germicidal UV is essential. *Photochemistry and Photobiology, 97*(3), 493–497. https://doi.org/10.1111/php.13421
4. Jacobs, N., Chan, K., Leso, V., D'Anna, A., Hollins, D., & Iavicoli, I. (2020). A critical review of methods for decontaminating filtering facepiece respirators. *Toxicology and Industrial Health, 36*(9), 654–680. https://doi.org/10.1177/0748233720964652
5. Cramer, A. K., Plana, D., Yang, H., Carmack, M. M., Tian, E., Sinha, M. S., Krikorian, D., Turner, D., Mo, J., Li, J., Gupta, R., Manning, H., Bourgeois, F. T., Yu, S. H., Sorger, P. K., & LeBoeuf, N. R. (2021). Analysis of SteraMist ionized hydrogen peroxide technology in the sterilization of N95 respirators and other PPE. *Scientific Reports, 11*(1), 2051. https://doi.org/10.1038/s41598-021-81365-7
6. Heimbuch, B. K., Wallace, W. H., Kinney, K., Lumley, A. E., Wu, C.-Y., Woo, M.-H., & Wander, J. D. (2011). A pandemic influenza preparedness study: Use of energetic methods to decontaminate filtering facepiece respirators contaminated with H1N1 aerosols and droplets. *American Journal of Infection Control, 39*(1), e1–e9. https://doi.org/10.1016/j.ajic.2010.07.004
7. Lore, M. B., Heimbuch, B. K., Brown, T. L., Wander, J. D., & Hinrichs, S. H. (2012). Effectiveness of three decontamination treatments against influenza virus applied to filtering facepiece respirators. *The Annals of Occupational Hygiene, 56*(1), 92–101. https://doi.org/10.1093/annhyg/mer054
8. Centers for Disease Control and Prevention. (2020, February 11). Implementing filtering facepiece respirator (FFR) reuse, including reuse after decontamination, when there are known shortages of N95 respirators. Centers for Disease Control and Prevention. Retrieved from https://www.cdc.gov/coronavirus/2019-ncov/hcp/ppe-strategy/decontamination-reuse-respirators.html. 28 Nov 2021.
9. Kowalski, W. (2009). *Ultraviolet germicidal irradiation handbook: UVGI for air and surface disinfection*. Springer. https://doi.org/10.1007/978-3-642-01999-9
10. Horton, L., Torres, A. E., Narla, S., Lyons, A. B., Kohli, I., Gelfand, J. M., Ozog, D. M., Hamzavi, I. H., & Lim, H. W. (2020). Spectrum of virucidal activity from ultraviolet to infrared radiation. *Photochemical & Photobiological Sciences, 19*(10), 1262–1270. https://doi.org/10.1039/D0PP00221F
11. Tseng, C.-C., & Li, C.-S. (2007). Inactivation of viruses on surfaces by ultraviolet germicidal irradiation. *Journal of Occupational and Environmental Hygiene, 4*(6), 400–405. https://doi.org/10.1080/15459620701329012
12. Pendyala, B., Patras, A., Pokharel, B., & D'Souza, D. (2020). Genomic modeling as an approach to identify surrogates for use in experimental validation of SARS-CoV-2 and HuNoV inactivation by UV-C treatment. *Frontiers in Microbiology, 11*, 572331. https://doi.org/10.3389/fmicb.2020.572331
13. Raeiszadeh, M., & Adeli, B. (2020). A critical review on ultraviolet disinfection systems against COVID-19 outbreak: applicability, validation, and safety considerations. *ACS Photonics, 7*(11), 2941–2951. https://doi.org/10.1021/acsphotonics.0c01245
14. World Health Organization. (2022). Global analysis of health care waste in the context of COVID-19. World Health Organization. Retrieved from https://www.who.int/publications-detail-redirect/9789240039612. 1 Mar 2022.
15. Bergman, M. S., Viscusi, D. J., Heimbuch, B. K., Wander, J. D., Sambol, A. R., & Shaffer, R. E. (2010). Evaluation of multiple (3-cycle) decontamination processing for filtering facepiece respirators. *Journal of Engineered Fibers and Fabrics, 5*(4), 33–41. https://doi.org/10.1177/155892501000500405
16. Paul, D., Gupta, A., & Maurya, A. K. (2020). Exploring options for reprocessing of N95 filtering facepiece respirators (N95-FFRs) amidst COVID-19 pandemic: A systematic review. *PLoS One, 15*(11), 1–24. https://doi.org/10.1371/journal.pone.0242474
17. Grist, S. M., Geldert, A., Gopal, A., Su, A., Balch, H. B., Herr, A. E., the N95DECON Consortium. (2021). Current understanding of ultraviolet-C decontamination of N95 filtering facepiece respirators. *Applied Biosafety, 26*(2), 90–102. https://doi.org/10.1089/apb.20.0051
18. Mills, D., Harnish, D. A., Lawrence, C., Sandoval-Powers, M., & Heimbuch, B. K. (2018). Ultraviolet germicidal irradiation of

influenza-contaminated N95 filtering facepiece respirators. *American Journal of Infection Control, 46*(7), e49–e55. https://doi.org/10.1016/j.ajic.2018.02.018

19. Heimbuch, B., & Harnish, D. (2019). Research to mitigate a shortage of respiratory protection devices during public health emergencies. Report to the United States Food and Drug Administration (FDA) No. HHSF223201400158C. Retrieved from https://www.ara.com/wp-content/uploads/MitigateShortageofRespiratoryProtectionDevices_3.pdf. 23 Nov 2021.
20. Ozog, D. M., Sexton, J. Z., Narla, S., Pretto-Kernahan, C. D., Mirabelli, C., Lim, H. W., Hamzavi, I. H., Tibbetts, R. J., & Mi, Q.-S. (2020). The effect of ultraviolet C radiation against different N95 respirators inoculated with SARS-CoV-2. *International Journal of Infectious Diseases, 100*, 224–229. https://doi.org/10.1016/j.ijid.2020.08.077
21. Fischer, R. J., Morris, D. H., van Doremalen, N., Sarchette, S., Matson, M. J., Bushmaker, T., Yinda, C. K., Seifert, S. N., Gamble, A., Williamson, B. N., Judson, S. D., de Wit, E., Lloyd-Smith, J. O., & Munster, V. J. (2020). Effectiveness of N95 respirator decontamination and reuse against SARS-CoV-2 virus. *Emerging Infectious Diseases, 26*(9), 2253–2255. https://doi.org/10.3201/eid2609.201524
22. Smith, J. S., Hanseler, H., Welle, J., Rattray, R., Campbell, M., Brotherton, T., Moudgil, T., Pack, T. F., Wegmann, K., Jensen, S., Jin, J., Bifulco, C. B., Prahl, S. A., Fox, B. A., & Stucky, N. L. (2020). Effect of various decontamination procedures on disposable N95 mask integrity and SARS-CoV-2 infectivity. *Journal of Clinical and Translational Science, 5*(1), e10. https://doi.org/10.1017/cts.2020.494
23. Simmons, S. E., Carrion, R., Alfson, K. J., Staples, H. M., Jinadatha, C., Jarvis, W. R., Sampathkumar, P., Chemaly, R. F., Khawaja, F., Povroznik, M., Jackson, S., Kaye, K. S., Rodriguez, R. M., & Stibich, M. A. (2021). Deactivation of SARS-CoV-2 with pulsed-xenon ultraviolet light: Implications for environmental COVID-19 control. *Infection Control & Hospital Epidemiology, 42*(2), 127–130. https://doi.org/10.1017/ice.2020.399
24. Golovkine, G. R., Roberts, A. W., Cooper, C., Riano, S., DiCiccio, A. M., Worthington, D. L., Clarkson, J. P., Krames, M., Zhang, J., Gao, Y., Zhou, L., Biering, S. B., & Stanley, S. A. (2021). Practical considerations for Ultraviolet-C radiation mediated decontamination of N95 respirator against SARS-CoV-2 virus. *PLoS One, 16*(10), e0258336. https://doi.org/10.1371/journal.pone.0258336
25. Rathnasinghe, R., Karlicek, R. F., Schotsaert, M., Koffas, M., Arduini, B. L., Jangra, S., Wang, B., Davis, J. L., Alnaggar, M., Costa, A., Vincent, R., García-Sastre, A., Vashishth, D., & Balchandani, P. (2021). Scalable, effective, and rapid decontamination of SARS-CoV-2 contaminated N95 respirators using germicidal ultraviolet C (UVC) irradiation device. *Scientific Reports, 11*(1), 19970. https://doi.org/10.1038/s41598-021-99431-5
26. Viscusi, D. J., King, W. P., & Shaffer, R. E. (2007). Effect of decontamination on the filtration efficiency of two filtering facepiece respirator models. *Journal of the International Society for Respiratory Protection, 24*, 15.
27. Viscusi, D. J., Bergman, M. S., Eimer, B. C., & Shaffer, R. E. (2009). Evaluation of five decontamination methods for filtering facepiece respirators. *Annals of Occupational Hygiene, 53*(8), 815–827. https://doi.org/10.1093/annhyg/mep070
28. Viscusi, D. J., Bergman, M. S., Novak, D. A., Faulkner, K. A., Palmiero, A., Powell, J., & Shaffer, R. E. (2011). Impact of three biological decontamination methods on filtering facepiece respirator fit, odor, comfort, and donning ease. *Journal of Occupational and Environmental Hygiene, 8*(7), 426–436. https://doi.org/10.1080/15459624.2011.585927
29. Lindsley, W. G., Martin, S. B., Thewlis, R. E., Sarkisian, K., Nwoko, J. O., Mead, K. R., & Noti, J. D. (2015). Effects of ultraviolet germicidal irradiation (UVGI) on N95 respirator filtration performance and structural integrity. *Journal of Occupational and Environmental Hygiene, 12*(8), 509–517. https://doi.org/10.1080/15459624.2015.1018518
30. Corman, V. M., Landt, O., Kaiser, M., Molenkamp, R., Meijer, A., Chu, D. K. W., Bleicker, T., Brünink, S., Schneider, J., Schmidt, M. L., Mulders, D. G. J. C., Haagmans, B. L., van Der Veer, B., van den Brink, S., Wijsman, L., Goderski, G., Romette, J. L., Ellis, J., Zambon, M., … Drosten, C. (2020). Detection of 2019 novel coronavirus (2019-nCoV) by real-time RT-PCR. *Eurosurveillance, 25*(3), 2000045.
31. Araujo, D. B., Machado, R. R. G., Amgarten, D. E., Malta, F. D. M., de Araujo, G. G., & Monteiro, C. O. (2020). SARS-CoV-2 isolation from the first reported patients in Brazil and establishment of a coordinated task network. *Memorias do Instituto Oswaldo Cruz, July*, 1–27. https://doi.org/10.1590/0074-02760200342.Running
32. Lo, C.-W., Matsuura, R., Iimura, K., Wada, S., Shinjo, A., Benno, Y., Nakagawa, M., Takei, M., & Aida, Y. (2021). UVC disinfects SARS-CoV-2 by induction of viral genome damage without apparent effects on viral morphology and proteins. *Scientific Reports, 11*(1), 13804. https://doi.org/10.1038/s41598-021-93231-7
33. Soler, M., Scholtz, A., Zeto, R., & Armani, A. M. (2020). Engineering photonics solutions for COVID-19. *APL Photonics, 5*(9), 090901. https://doi.org/10.1063/5.0021270
34. Sender, R., Bar-On, Y., Gleizer, S., & Milo, R. (2021). The total number and mass of SARS-CoV-2 virions. *National Academy of Science, 118*(25), e2024815118. https://doi.org/10.1073/pnas.2024815118
35. Pan, Y., Zhang, D., Yang, P., Poon, L. L. M., & Wang, Q. (2020). Viral load of SARS-CoV-2 in clinical samples. *The Lancet Infectious Diseases, 20*(4), 411–412. https://doi.org/10.1016/S1473-3099(20)30113-4
36. Wölfel, R., Corman, V. M., Guggemos, W., Seilmaier, M., Zange, S., Müller, M. A., Niemeyer, D., Jones, T. C., Vollmar, P., Rothe, C., Hoelscher, M., Bleicker, T., Brünink, S., Schneider, J., Ehmann, R., Zwirglmaier, K., Drosten, C., & Wendtner, C. (2020). Virological assessment of hospitalized patients with COVID-2019. *Nature, 581*(7809), 465–469. https://doi.org/10.1038/s41586-020-2196-x
37. Goyal, A., Reeves, D. B., Cardozo-Ojeda, E. F., Schiffer, J. T., & Mayer, B. T. (2020). Wrong person, place and time: Viral load and contact network structure predict SARS-CoV-2 transmission and super-spreading events [Preprint]. *Infectious Diseases (except HIV/AIDS)*. https://doi.org/10.1101/2020.08.07.20169920
38. Liao, L., Xiao, W., Zhao, M., Yu, X., Wang, H., Wang, Q., Chu, S., & Cui, Y. (2020). Can N95 respirators be reused after disinfection? How many times? *ACS Nano, 14*(5), 6348–6356. https://doi.org/10.1021/acsnano.0c03597
39. Ontiveros, C. C., Sweeney, C. L., Smith, C., MacIsaac, S., Bennett, J. L., Munoz, S., Stoddart, A. K., & Gagnon, G. A. (2021). Assessing the impact of multiple ultraviolet disinfection cycles on N95 filtering facepiece respirator integrity. *Scientific Reports, 11*(1), 12279. https://doi.org/10.1038/s41598-021-91706-1
40. Huber, T., Goldman, O., Epstein, A. E., Stella, G., & Sakmar, T. P. (2021). Principles and practice for SARS-CoV-2 decontamination of N95 masks with UV-C. *Biophysical Journal, 120*(14), 2927–2942. https://doi.org/10.1016/j.bpj.2021.02.039
41. CDC. (2020, June 4). 42 CFR Part 84 respiratory protective devices. CDC's National Institute of Occupational Safety and Health (NIOSH). Retrieved from https://www.cdc.gov/niosh/npptl/topics/respirators/pt84abs2.html
42. Cook, T. M. (2020). Personal protective equipment during the coronavirus disease (COVID) 2019 pandemic—A narrative review. *Anaesthesia, 75*(7), 920–927. https://doi.org/10.1111/anae.15071
43. Chandran, K. M., Praveen, C. R., Kanjo, K., Narayan, R., & Menon, R. (2021). Efficacy of ultraviolet-C devices for the disinfection of personal protective equipment fabrics and N95 respirators. *Journal of Research of the National Institute of Standards and Technology, 126*, 126023. https://doi.org/10.6028/jres.126.023

Authors and Affiliations

Patrícia Metolina[1] · Lilian Gomes de Oliveira[2] · Bruno Ramos[1] · Yan de Souza Angelo[2] · Paola Minoprio[2] · Antonio Carlos Silva Costa Teixeira[1]

✉ Patrícia Metolina
pmetolina@usp.br

✉ Antonio Carlos Silva Costa Teixeira
acscteix@usp.br

[1] Research Group in Advanced Oxidation Processes (AdOx), Chemical Systems Engineering Center-Department of Chemical Engineering, University of São Paulo, São Paulo, Brazil

[2] Scientific Platform Pasteur USP (SPPU), University of São Paulo, São Paulo, Brazil